Energy Equip. Sys./ Vol. 7/No. 3/Sep. 2019/ 271-278

ENERGY EQUIPSYS

Energy Equipment and Systems

http://energyequipsys.ut.ac.ir
www.energyequipsys.com

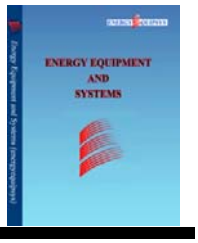

Reaching the betz limit experimentally and numerically

Authors

Mohammad Hassan Ranjbar [a]
Seyyed Abolfazl Nasrazadani [a]
Hadi Zanganeh Kia [a]
Kobra Gharali [a,b*]

[a] College of Mechanical Engineering, Faculty of Engineering, University of Tehran, Tehran, Iran

[b] Waterloo Institute for Sustainable Energy (WISE), University of Waterloo, Waterloo, ON, N2L 3G1, Canada

Article history:

Received : 3 December 2018
Accepted : 13 July 2019

ABSTRACT

The Betz theory expresses that no horizontal axis wind turbine can extract more than 16/27 (59.3%) of the kinetic energy of the wind. The factor 16/27 (0.593) is known as the Betz limit. Horizontal Axis wind turbine designers try to improve the power performance to reach the Betz limit. Modern operational wind turbines achieve at peak 75% to 80% of the Betz limit. In 1919, Albert Betz used an analytical method to derive the Betz limit. He derived momentum equations of an Actuator Disc (AD) in the stream. In this research, an experimental and a numerical setup based on the Actuator Disc (AD) have been designed and tested to reach the Betz limit. A Plexiglass screen with the porosity of 0.5 mimics the wind turbine rotor. For the numerical study, a 2D flow filed is considered. The results of both experimental and numerical methods agree well with the analytical results of the Betz theory. From the experimental and numerical results, the relative errors in comparison with the Betz limit (which is 16/27) are 0.16% and 1.27%, respectively. The small amount of errors shows the possibility of reaching the Betz limit using either experimental or numerical methods. This approach can be used for modeling ideal wind turbines, ideal rotating devices or ideal wind farms either numerically or experimentally and gives the maximum possible power extractions; thus, any improvement to the performance of a system can be made by this method.

Keywords: Betz Limit, Actuator Disc, Wind Turbine, CFD, Experiment, Porosity.

1. Introduction

In 2017, the global installed wind turbine capacity was increased 22 times Compared to 2001 [1]. This notable growth of power extraction from wind energy motivates researchers to increase the performance of wind turbines based on the demand. Some basic theories have been developed and modified. Actuator Disc (AD) Theory is one of the most famous ones. It was used by Rankine [2] and Froude [3, 4] by assumption of ideal and laminar flows. In 1919, Betz proved the impossibility of energy extraction more than 16/27 (59.3%) of the available wind kinetic energy based on the AD theory [5]. Lanchester [6] and Joukowsky [7] found the same results independently; the theory was called Lanchester–Betz–Joukowsky limit or briefly Betz limit. Betz assumed an infinite number of rotor blades under an axial and incompressible flow; also, a uniform thrust was exerted on the disc with no drag force. Recent operational wind turbines can achieve 75% to 80% of the Betz limit value at peak power generation [8].
When the power coefficient of a wind turbine becomes close to the Betz limit

* Corresponding author: Kobra Gharali
-College of Mechanical Engineering, Faculty of Engineering, University of Tehran, Tehran, Iran
-Waterloo Institute for Sustainable Energy (WISE), University of Waterloo, Waterloo, ON, N2L 3G1, Canada
Email: kgharali@ut.ac.ir & kgharali@uwaterloo.ca

value, the design can be identified as an ideal design. Jiang et al. [9] by blade element momentum (BEM) showed that in order to reach 59.3% of the total available power, the tip speed ratio should be infinity which is impossible. Lellis et al. [10] suggested that the Betz limit should hold true for any device that harvests power through drag or torque in a horizontal-axis rotational motion perpendicular to the wind direction. Also, they claimed the Betz limit is valid for Loyd's drag power Airborne Wind Energy (AWE) systems. All of their claims were supported by physical principles and mathematical formulations.

In the literature, the rotor of a wind turbine can be replaced by a porous disc for modeling the wind turbine pressure drop and the wake of the rotor. One of the main parameters for wind turbines is *solidity* which can be replaced by porosity in porous discs. Porosity is the ratio of the void space to the total area of the disc; the solidity is the ratio of covered or engaged space to the total area of the disc. One can increase the blade number to the infinity and assumes the rotor as a porous disc. Aubrun et al. [11] measured the coefficients of power and thrust experimentally for the porosity range of 55% to 70% in 2007. They made the discs from some circular wire meshes and tested them under a constant wind speed to study the wake characterization of a wind turbine. Theunissen et al. [12] analyzed an offshore wind farm experimentally using circular porous discs. For the shape of the porous discs, they made some holes on the discs for achieving the same velocity of the wake that they expected. Sforza et al. [13] studied the wind turbine wakes. They showed that when the same thrust coefficients are exerted on a real turbine and a porous disc, the wake characteristics of both will be the same. They used perforated discs of different porosities to simulate a range of rotor thrust loadings. Dighe et al. [14] studied a diffuser augmented wind turbine by the AD approach. They installed selected porous discs in the middle of the diffuser. With the porosity of 40%, they get the same thrust coefficients of real rotors. They continued their studies and showed the effects of Gurney flaps on the diffuser augmented wind turbines by using the porosity of 70% and compared the results with those of a case without any Gurney flap. In this research, the porous disc was a cheap and robust tool to analyze the effect of the Gurney flap [15]. Auburn et al. [16] compared a non-rotating turbine model with a rotating one with the same coefficient of thrust.

The scale of the model was about 1:300. They measured the velocity deficit of the wake. Lignarolo et al. [17] made a comparison between a turbine and an AD model using Particle Image Velocimetry (PIV) technique. Their results were very close in terms of power, enthalpy, and thrust. Aloui et al. [18] used PIV and Proper Orthogonal Decomposition (POD) methods to investigate the wake characteristics by a porous disc with a porosity of 55%. Charmanski et al. [19] studied boundary layers for a wind turbine array by using some discs with the porosity of 51%. The porosity value was chosen based on the drag coefficient extracted from a real rotating wind turbine.

In some studies in particular wind farms, installing discs that show the minimum energy lost are helpful. The aim of this study is showing the possibility of achieving the Betz limit value. To reach this ideal power extraction device a numerical simulation and an experimental setup are designed.

2. The Betz Limit

In order to calculate the maximum theoretical efficiency of a thin rotor, the rotor can be replaced by a stationary disc or an actuator disc (AD). The disc extracts energy from the stream passing through it. Ideal conditions such as frictionless flows, and no rotational velocity in the wake should be assumed. The disc works like a drag device that reduces the velocity. The general momentum theory showing the performance of the disc is [20]

$$C_P = \frac{P}{\frac{1}{2}\rho U_\infty^3 A_D} = 4a(1-a)^2. \quad (1)$$

In Eq. 1, P, ρ, U_∞ and A_D are power, density, wind velocity and disc area, respectively. It means the coefficient of performance (C_P) is a quadratic function of the induction factor (a) where the induction factor is

$$a = \frac{(U_\infty - U_w)}{U_\infty}. \quad (2)$$

In this assumption U_∞ and U_w are the wind speed and the wake velocity in the proximity of the disc, respectively. The maximum value of C_P is obtained from the extremum value of the Eq. (1). That is

$$\frac{dC_P}{da} = 4(1-a)(1-3a) = 0. \quad (3)$$

If $= \frac{1}{3}$, the maximum $C_{P_{max}}$ is

$$C_{P_{max}} = \frac{16}{27} = 0.\overline{592}. \quad (4)$$

This maximum power coefficient is the Betz limit or the 16/27 value.

3. Experimental setup

Experiments were performed in an open-loop wind tunnel facility at the University of Tehran. The dimensions of the wind tunnel nozzle exit are 0.5× 0.5 m^2. The tunnel can operate at a maximum speed of 15 m/s. For measuring the average downstream velocity of the screens, the anemometer YK-2005AM was used in the proximity of the disc (Fig. 1). Free-stream velocity, U, was measured from 4 to 13 m/s with and without the screen (disc). In total, seven cases with different velocities have been tested.

The Plexiglass screens (discs) with the Solidity (S) of 0.5 were cut with a laser ($\pm 0.1\ mm$). Different solidities were tested. Using a trial and error process, the solidity of 0.5 provided a good agreement with the theory. The disc was made by long rectangular blocks, Fig. 2, similar to the 2D assumption of the Betz theory.

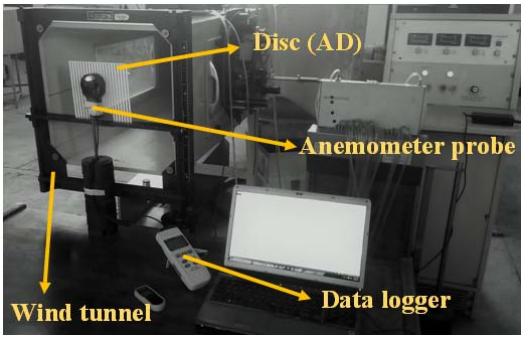

Fig. 1. Experimental setup located in the Fluid Mechanic Lab of Mechanical Engineering Department, University of Tehran.

The dimensions of the disc, the thickness and the width of the square plexiglass screen are equal, h=z=3mm (Fig. 3).

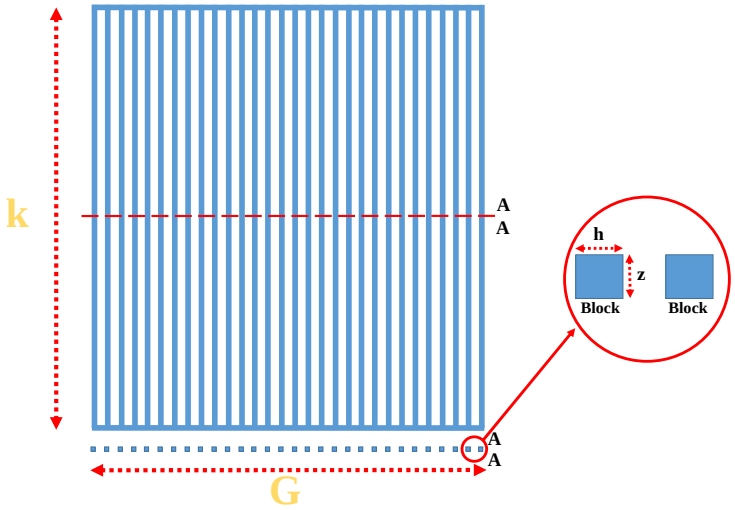

Fig. 2. Parameters of the disc

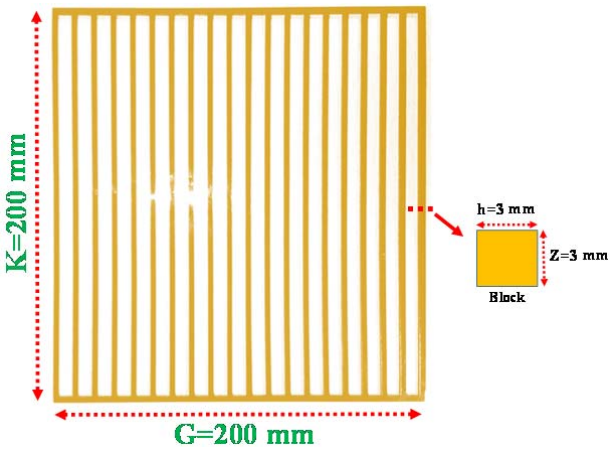

Fig. 3. Dimensions of the disc

4.Numerical Setup

4.1. Governing equations

The governing equations, continuity and incompressible Navier-Stokes equations, in tensor notations, are

$$\frac{\partial v_i}{\partial x_i} = 0 \,, \tag{5}$$

$$\rho \frac{\partial v_i}{\partial t} + \rho \frac{\partial (v_i v_j)}{\partial x_j} = -\frac{\partial P}{\partial x_i} + \mu \left(\frac{\partial^2 v_i}{\partial x_j^2} + \frac{\partial^2 v_j}{\partial x_j \partial x_i} \right) + G_i \,, \tag{6}$$

where v, ρ, P and μ denote velocity, fluid density, mean static pressure and dynamic viscosity, respectively. In these equations, term G (body forces) is neglected.

4.2. Geometry and mesh

For the 2D simulation of the disc, small squares similar to Fig. 2 are used, causing a pressure drop across the disc. Fig. 4 shows the cross-sectional view (x-y plane) of the screen (2D).

To get a mesh independent solution, five different meshes, from 15000 to 100000 elements were generated. The criteria for the mesh selection is based on the mean velocity in the proximity of the disc. The selected grid of 6.8x 10^4 elements was used. The size of the first layer is 0.01 mm with a 1.2 growth rate and the maximum cell size of 35mm. These settings have been used to generate unstructured grids while y+ < 8.

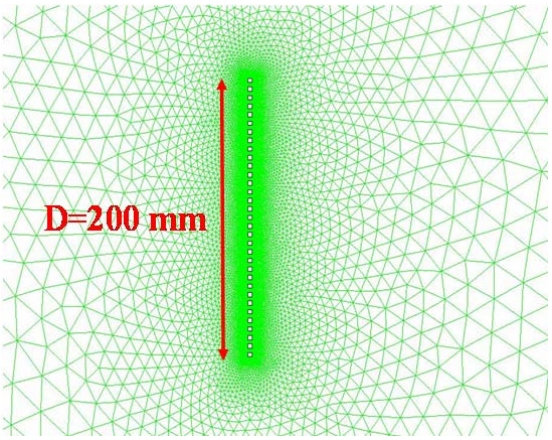

Fig. 4. The cross-sectional view of the AD I (2D simulation).

C_P

4.3. Solver

For the boundary layer conditions, the inlet (left side in Fig. 5) and the outlet (right side in Fig. 5) are assumed velocity inlet and pressure outlet, respectively. The upper and bottom boundaries are considered symmetric (Fig. 5). The inlet velocity varies from 4 to 13 m/s. The Partial Differential Equations (Eq. 5 and Eq. 6) have been solved based on the SIMPLE algorithm with the aid of k-ω turbulence model. The second-order upwind spatial discretization is used. The flow is assumed 2D, steady and incompressible. The convergence criteria were set 10^{-3} for all the residuals. In the next section, for the validation, the numerical results are compared with the Betz theory and the experimental results.

5.Results and discussion

5.1. Induction factor, a

Figure 6 shows the induction factor *a* (Eq. 2) for different inlet velocities experimentally and numerically. The velocities are non-dimensional($\frac{V}{V_{ref}}$, where V_{ref} is 8 m/s).

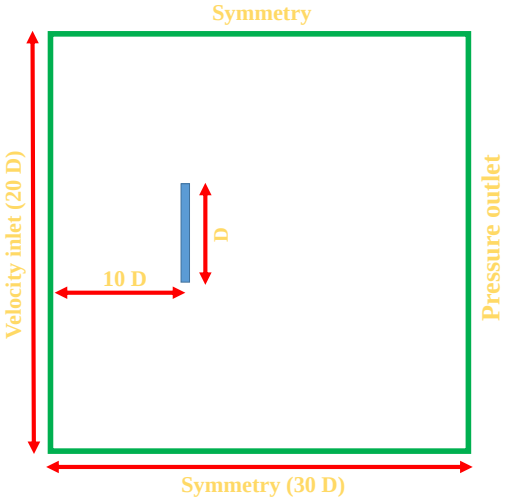

Fig. 5. CFD solution domain and the boundary conditions

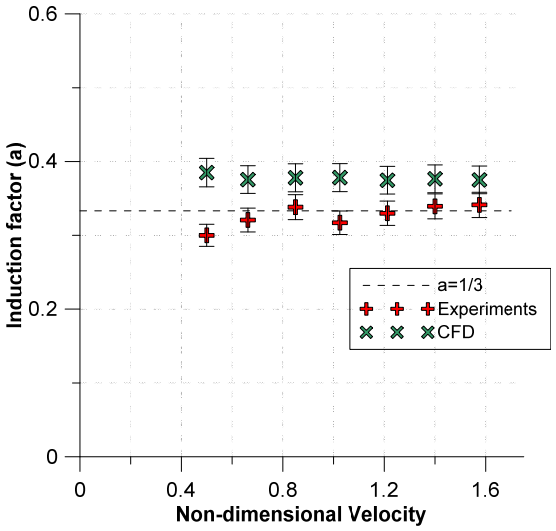

Fig. 6. Variations of induction factor (a) versus velocity

In Fig. 6, the average value of induction factor from experimental and CFD results are 0.326 and 0.377, respectively. From Eq. 3, the optimum induction factor in generating the highest performance coefficient is 1/3.

5.2. Performance coefficient

The results of the performance coefficient (C_P) are illustrated in Fig. 7. From Eq. 4, the maximum value of the C_P is 16/27 (the Betz limit). The average values of C_P are 0.5916 and 0.5850 from the experimental and CFD results, respectively. The average deviations from the Betz limit are 0.16% and 1.27% experimentally and numerically, respectively. The maximum deviations are related to low wind speeds or low Reynolds numbers. Reynolds number is defined as $Re = \frac{\rho V G}{\mu}$, where G is the disc dimension (Fig. 2) and μ is viscosity. The low errors show that the results from the designed experiment setup and the numerical simulation agree well with the Betz theory. It is possible to reach the Betz limit value numerically and experimentally by using proper assumptions.

5.3. Pressure drop and velocity deficit

A rotor of a wind turbine replaced by a disc results in pressure drop and velocity deficit in the domain. In Fig. 8, the low-velocity region (blue color) in the downwind of the disc shows velocity deficit. In this figure, the wind speed is 12.6 m/s.

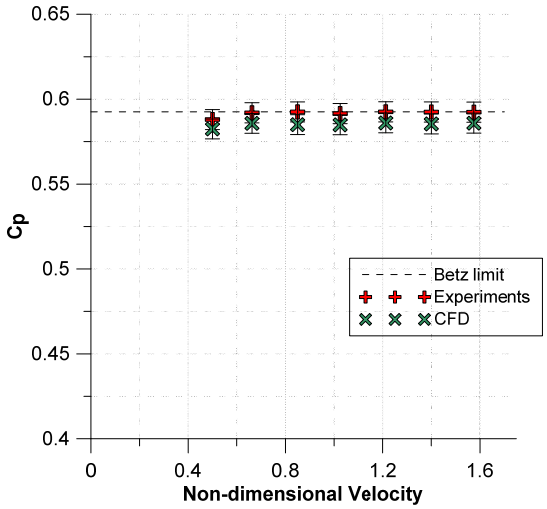

Fig. 7. Variations of Cp versus velocity

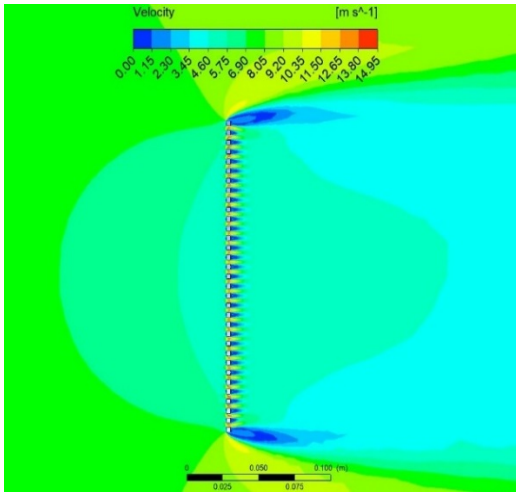

Fig. 8. Velocity contours, upstream and downstream of the disc

Figure 9 illustrates the pressure drop in the disc with the inlet wind speed of 8m/s. Both of these figures agree well with the Betz theory.

6. Conclusions

An experimental setup and a numerical simulation were designed and tested based on the Actuator Disc, AD theory. The aim is to reach the Betz limit. The disc was made from Plexiglass screens. After some trial and errors, the solidity of the disc was selected as 0.5. SIMPLE algorithm with the aid of k-ω turbulence model was used for the numerical solution. In numerical simulation, a line of squares simulated the cross-section of the disc for a 2D domain. The results from either the experimental study or the numerical one had a good agreement. The results also were overlapped with the analytical results from the Betz theory. For the low wind speeds or low Reynolds numbers, the induction factor and the performance coefficient deviated slightly from the ideal value in both numerical and experimental methods. Increasing the Reynolds number resulted in reaching the Betz limit. The performance coefficient errors in comparison with the Betz limit (which is 16/27) were 0.16% and 1.27% from the experimental results and CFD results, respectively. Then, it is possible to reach the Betz limit either experimentally or numerically by using a thin disc with a solidity of 0.5. This approach can be used for modeling ideal wind turbines, ideal rotating devices or ideal wind farms either numerically or experimentally. This method gives the maximum possible power extractions; thus, any improvement to the performance of a system can be made by this method. For example, the performance of a novel design of a wind turbine may pass the Betz limit; with the aid of the mentioned method, it is possible to estimate the maximum power enrichment.

Acknowledgment

The authors would like to acknowledge the help rendered by *Dr. A. Ashrafizadeh*, Faculty of Mechanical Engineering, K. N. Toosi University of Technology, Tehran, Iran, for sharing some of the test facilities with us.

References

[1]Global Wind Statistics (GWEC) report 2017.
[2]Rankine, W. J., Transactions, Institute of Naval Architects, Vol. 19, P. 47, 1878.
[3]Froude, W., Transactions, Institute of Naval Architects, Vol. 6, P. 13, 1865.
[4]Froude, R. E., Transactions, institute of Naval Architects, Vol. 30, P. 390, 1889.
[5]Betz, A. (1920). Theoretical limit for best utilization of wind by wind-motors. Magazine for the Entire Turbine System, 20, 307-309.
[6]Lanchester, F. W. (1915). A contribution to the theory of propulsion and the screw

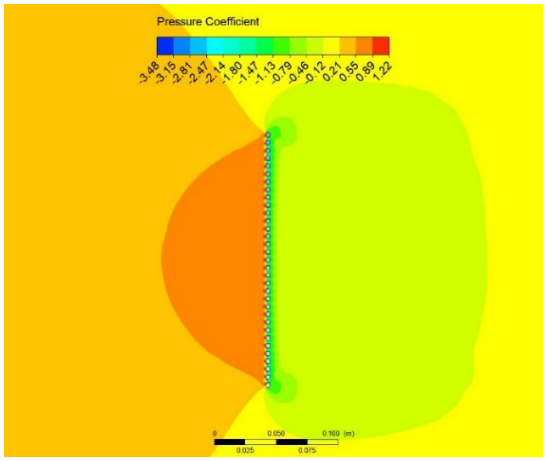

Fig. 9. Pressure coefficient contours

propeller. Naval Engineers Journal, 27(2), 509-510.

[7]Joukowsky NE. Windmill of the NEJ type. Transactions of the Central Institute for Aero-Hydrodynamics of Moscow, 1920. Also published in Joukowsky NE. Collected Papers Vol VI. The Joukowsky Institute for AeroHydrodynamics, Moscow: vol VI, 405–409, 1937 (in Russian).

[8] Tony Burton et al., (ed), Wind Energy Handbook, John Wiley and Sons 2001 ISBN 0471489972 page 65.

[9]Jiang, H., Li, Y., & Cheng, Z. (2015). Performances of ideal wind turbine. Renewable Energy, 83, 658-662.

[10]De Lellis, M., Reginatto, R., Saraiva, R., & Trofino, A. (2018). The Betz limit applied to Airborne Wind Energy. Renewable Energy, 127, 32-40.

[11]Aubrun, S., Devinant, P., & Espana, G. (2007, May). Physical modeling of the far wake from wind turbines. Application to wind turbine interactions. In Proceedings of the European wind energy conference, Milan, Italy (pp. 7-10).

[12]Theunissen, R., Housley, P., Allen, C. B., & Carey, C. (2015). Experimental verification of computational predictions in power generation variation with layout of offshore wind farms. Wind Energy, 18(10), 1739-1757.

[13]PM Sforza, S., & Smorto, M. (1981). Three-dimensional wakes of simulated wind turbines. AIAA Journal, 19(9), 1101-1107.

[14]Dighe, V. V., Avallone, F., & van Bussel, G. J. W. (2016). Computational study of diffuser augmented wind turbine using AD force method. International Journal of Computational Methods and Experimental Measurements,4(4), 522-531.

[15]Dighe, V. V., Avallone, F., Tang, J., & van Bussel, G. (2017). Effects of Gurney Flaps on the Performance of Diffuser Augmented Wind Turbine. In 35th Wind Energy Symposium (p. 1382).

[16]Aubrun, S., Loyer, S., Hancock, P. E., & Hayden, P. (2013). Wind turbine wake properties: Comparison between a non-rotating simplified wind turbine model and a rotating model.Journal of Wind Engineering and Industrial Aerodynamics,120, 1-8.

[17]Lignarolo, L. E. M., Ragni, D., Ferreira, C. J., & Van Bussel, G. J. W. (2016). Experimental comparison of a wind-turbine and of an actuator-disc near wake. Journal of Renewable and Sustainable Energy, 8(2), 023301.

[18]Aloui, F., Kardous, M., Cheker, R., & Nasrallah, S. B. (2013). Study of the wake induced by a porous disc. In 21 st Congress Francais de Mecanique.

[19]Charmanski, K., Turner, J., & Wosnik, M. (2014, August). Physical model study of the wind turbine array boundary layer. In ASME 2014 4th Joint US-European Fluids Engineering Division Summer Meeting collocated with the ASME 2014 12th International Conference on Nanochannels, Microchannels, and Minichannels (pp. V01DT39A010-V01DT39A010). American Society of Mechanical Engineers.

[20]Manwell, J. F., McGowan, J. G., & Rogers, A. L. (2010). Wind energy explained: theory, design and application. John Wiley & Sons.